

# Pre-Procedural MRI and 3D Finite Element Modeling for Prediction of Irreversible Electroporation Ablation Zones in a Rat Liver Tumor Model

Y. Zhang<sup>1,2</sup>, H. M. Al-Angari<sup>3</sup>, Y. Guo<sup>2</sup>, J. Nicolai<sup>2</sup>, R. A. Klein<sup>2</sup>, A. V. Sahakian<sup>3</sup>, R. A. Omary<sup>2,4</sup>, and A. C. Larson<sup>2,4</sup>

<sup>1</sup>Bioengineering, University of Illinois at Chicago, Chicago, IL, United States, <sup>2</sup>Radiology, Northwestern University, Chicago, IL, United States, <sup>3</sup>Electrical Engineering and Computer Science, Northwestern University, Evanston, IL, United States, <sup>4</sup>Robert H. Lurie Comprehensive Cancer Center, Northwestern University, Chicago, IL, United States

## INTRODUCTION

Irreversible electroporation (IRE) [1] has recently been applied as a novel tissue ablation modality; IRE involves application of short-lived electrical fields across the cell membrane to permanently increase membrane permeability leading to cell death. 2D finite element methods (FEM) are used to model anticipated electrical field distributions but these typically assume homogeneous tissue conductivity [2]; heterogeneity could lead to poor approximations of subsequent ablation volume. In this work, we developed a 3D FEM approach using pre-procedural MRI measurements to produce a patient-specific 3D surrogate-conductivity map for simulation of IRE ablation zones in a rat model of hepatocellular carcinoma (HCC). The purpose of this study was to prospectively test the hypothesis that pre-procedural MRI and 3D FEM can be used to accurately predict IRE ablation zones.

## MATERIALS AND METHODS

**Tumor Cell Culture and Animal Model** 16 Sprague-Dawley rats were used for our ACUC-approved experiments. The N1-S1 HCC cell line was used to grow one tumor in each rat; rats were divided into small (<8.50 mm, Group A) and large (> 8.50 mm, Group B) tumor size groups (8 rats/group). After anesthesia, rats were restrained in supine position and the liver exposed with midline incision. Two parallel platinum-iridium needle electrodes were inserted into the liver to straddle tumor centroid. **MRI Measurements** All experiments were performed using a 1.5T clinical MR scanner (Magnetom Espree, Siemens Medical Solutions) with a head coil. We acquired T2-weighted (T2W) turbo spin echo (TSE) images with repetition time/echo time (TR/TE) = 3640/61ms, flip angle = 150°, bandwidth = 205 Hz/pixel along the orientation parallel and perpendicular to the electrodes.

**IRE Procedures** After MRI scans, rats were removed from the scanner bore but remained fixed in supine position. Electrodes were connected to IRE function generator (ECM830). 2000V square wave pulses were applied (same protocol for 2 groups: 8 pulses, 100  $\mu$ s for the duration of 1 pulse and 100ms for the interval between 2 pulses). **Histology** After IRE procedure, rats were survived for 24 hours and the euthanized to harvest liver. Liver specimens were fixed in formalin and stained using hematoxylin and eosin (H&E). ImageJ (NIH) was used to manually draw a region-of-interest (ROI) circumscribing areas of cellular necrosis within each image to measure the resulting total ablation zone and non-ablated tumor zone for each animal.

**FEM Simulation** T2W images along the orientation parallel to the electrodes were manually segmented into normal liver and tumor region ROI, for each slice these ROI were a 2D structured matrix with MATLAB software (MathWorks, Natick, MA). Each 2D structured matrix was imported into COMSOL software (Comsol, Burlington, MA) with the slice stack combined to generate a 3D data volume via linear interpolation. Normal liver regions were assigned a conductivity value of 0.125 S/m whereas tumor tissues were assigned a value of 0.275 S/m [3]. The electrical field distribution map was generated based on this model, electrode position (identified within the MRI image stack), and applied IRE pulse parameters. The threshold for IRE in liver was assumed to be 60.0 V/mm. We measured the total area of IRE ablation and non-ablated tumor zones within these FEM simulations at central axial slice through the tumor. **Statistical Analysis** Pearson correlation coefficients were calculated to examine the relationship between FEM-simulated and histology-confirmed ablation zone measurements and a t-test was performed to compare the difference between untreated remnant tumor zone between large and small tumor treatment groups ( $p < 0.05$  considered statistically significant).

## RESULTS

FEM-simulated (Fig.1E) and histology-confirmed (Fig.1F) total ablation zones tended to cover the entire tumor region for Group A. However, ablation zones (Fig.2E and Fig.2F) tended to cover only a portion of the tumor for Group B rats. FEM-simulated total ablation zones were well correlated to histology-confirmed total ablation zones ( $r = 0.817$ ,  $p < 0.001$ ); the size of FEM-simulated untreated tumor zones was also well correlated with histology-confirmed viable remnant tumor zones ( $r = 0.781$ ,  $p < 0.001$ ). Untreated remnant tumor zones for Group A were significantly smaller than those in Group B ( $p = 0.007$ ).

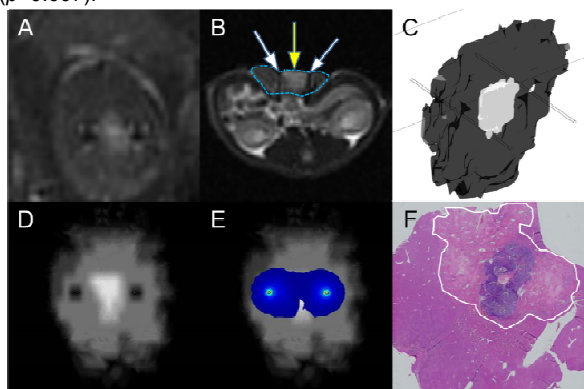


**Figure 1.** Representative images for Group A (left). T2W images (A and B, blue dashed circle for liver, white arrows for electrodes and yellow arrow for tumor), reconstructed 3D liver and tumor (C), axial view of 3D model (D), FEM simulated ablation zone (E, blue region) and histology-confirmed ablation zone (F, white circle).

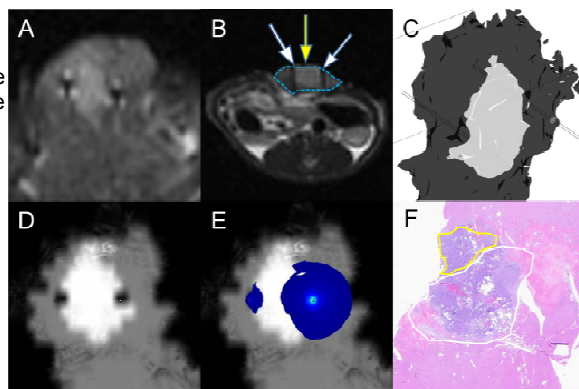


**Figure 2.** Representative images for Group B. (above) T2W images (A and B, blue dashed circle for liver, white arrows for electrodes and yellow arrow for tumor), reconstructed 3D liver and tumor (C), simulated ablation zone (E, blue region) and histology-confirmed ablation zone (F, white circle). Yellow circle indicated untreated tumor growing into surrounding normal liver.

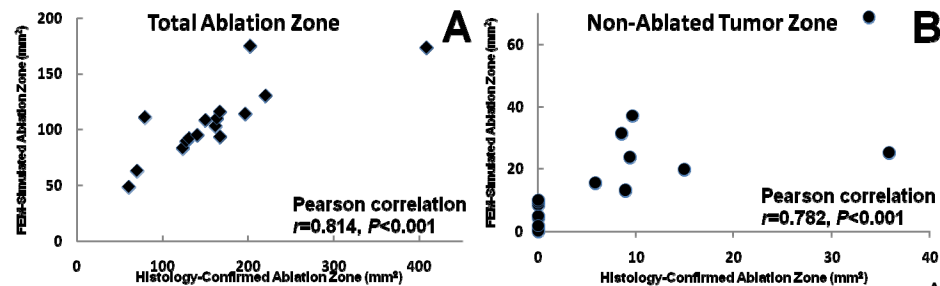


**Figure 3.** Scatterplots show the relationship between FEM-simulated IRE ablation zone and histology-confirmed IRE ablation zones.

## CONCLUSION

MRI and 3D FEM can be used to predict IRE ablation zones. These methods should permit pre-procedural, patient-specific optimization of IRE parameters (voltage and electrode positions) to ensure complete treatment of targeted lesions.

**Acknowledgments:** This work was made possible by CA134719 from National Cancer Institute and UL1 RR025741 from National Center for Research Resources (NCRR), both components of National Institutes of Health (NIH), and NIH Roadmap for Medical Research. **Reference:** [1]. Rubinsky et al. Technol Cancer Res Treat 2007;6:37-48 [2]. Davalos et al. Annals of Biomedical Engineering, 2005;33(2):223-231 [3]. Haemmerich et al. Physiol. Meas. 24 (2003) 251-260